Volume 1 | Number 1 | Jan 2013 | Pages 1–100

Nanoscale

www.rsc.org/nanoscale

ARTICLE TYPE

Molecular Resonant Dissociation of Surface-Adsorbed Molecules by Plasmonic Nanoscissors

Zhenglong Zhang,[a,b,c] Shaoxiang Sheng,[a] Hairong Zheng,[b] Hongxing Xu,[a] Mengtao Sun [a,*]

The ability to break individual bonds or specific modes in chemical reactions is an ardently sought goal by chemists and physicists. While photochemistry-based methodologies are very successful in controlling e.g. photocatalysis, photosynthesis and the degradation of plastic, it is hard to break individual molecular bonds for those molecules adsorbed on surface because of the weak light-absorption in molecules and the
10 redistribution of the resulting vibrational energy both inside the molecule, and to its surrounding environment. Here we show how to overcome these obstacles with plasmonic hot-electron mediated process and demonstrate a new method that allows the sensitive control of resonant dissociation of surface-adsorbed molecules by 'plasmonic' scissors. To that end, we used a high-vacuum tip-enhanced Raman spectroscopy (HV-TERS) setup to dissociate resonantly-excited NC_2H_6 fragments from Malachite
15 Green. The surface plasmons (SPs) excited at the sharp metal tip not only enhance the local electric field to harvest the light incident from the laser, but crucially supply 'hot electrons' whose energy can be transferred to individual bonds. These processes are resonant Raman, which result in active some chemical bonds, and then weaken these bonds, followed by dumping in lots of indiscriminant energy and breaking the weakest bond. The method allows for sensitive control of both the rate and probability of
20 dissociation through their dependence on the density of hot electrons, which can be manipulated by tuning the laser intensity or tunneling current/bias voltage in the HV-TERS setup, respectively. The concepts of plasmonic scissors open up new versatile avenues for the deep understanding of in situ surface-catalyzed chemistry.

1 Introduction

25 Developing methodologies that enable mode-specificity chemistry is a very important goal for chemists and an active field of study in the area of molecular reaction dynamics.[1, 2] One promising avenue for realizing vibration-resolved resonant dissociation relies on the excitation and control of molecular
30 vibrations. However, controlling vibrational modes for chemical reactions is challenging because of intramolecular vibrational energy redistribution[1, 3] (IVR) within an excited molecule on a picosecond timescale. For molecules in a gas, bond-breaking of molecular bonds can be induced and controlled by feedback-
35 optimized phase-shaped femtosecond laser pulses.[2] But for surface-adsorbed molecules the situation is significantly complicated by the dissipation of energy to the surrounding surface atoms, which take up the energy and thwart the bond-breaking process. Recent efforts have tried to address this issue
40 by using a laser to vibrationally excite C–H bonds in a gas-phase beam of triply-deuterated methane molecules in such a way that the C–H bonds would break as the molecules glance off a metal surface.[4] However, the challenge still remains as to how to achieve efficient, resonance excitation by laser and dissociation
45 by hot electrons for molecules adsorbed on a solid surface, prior

to the timescale of IVR, and energetic redistribution between the adsorbates and their environment. Vibrational mode specific bond dissociation in a single molecule have been performed by tunneling electrons from a scanning tunneling microscope
50 (STM),[5, 6] but we herein focus on the plasmon-driven resonantly excited vibration-resolved resonant dissociations by plasmonic hot electrons as plasmonic scissors in STM-based tip-enhanced Raman spectroscopy (TERS).

Recent reports have shown that hot electrons generated from
55 plasmon decay (Landau damping)[7-9] can play an important role in surface chemical reactions.[9-17] Very recently, surface catalytic reaction in TERS has been expected,[16, 18, 19] and the molecular dimerization in TERS have been successfully realized experimentally. Plasmon scissors for molecular designs have been
60 reported in TERS and SERS experiments,[20, 21] where hot electrons (generated from plasmon decay)break the weakest – N=N– bond of DMAB. While the Raman spectra were not bond-selectively resonant excited (they are normal Raman). Recently, the concept of plasmon-driven selective bond activation has been
65 proposed.[22, 23] The hot electrons transfer to molecules adsorbed on the substrate, and thereby induced electron-driven bond dissociation.[22, 23] Firstly, hot electrons are attached temporally to the PES of molecule, which transiently charges the neutral PES to negative PES and decreases the reaction barrier. Secondly, the

reaction energy can be excited to be higher than or close to the dissociation energy by laser. Then, the high kinetic energy of the hot electrons provides the additional energy required for dissociation of the active bonds.[11, 17, 20, 22, 23] Here we show how hot electrons generated from the plasmon decay in the nanogap of a high-vacuum TERS (HV-TERS) setup (see Fig. 1) can be used to dissociate the resonantly excited Malachite Green (MG) adsorbed on Ag and Au surfaces with sensitive control of the dissociation rate and probability through tuning of the hot electron density. These processes are resonant Raman to active some chemical bonds, and then weaken these bonds, followed by dumping in lots of indiscriminant energy and breaking the weakest bond.
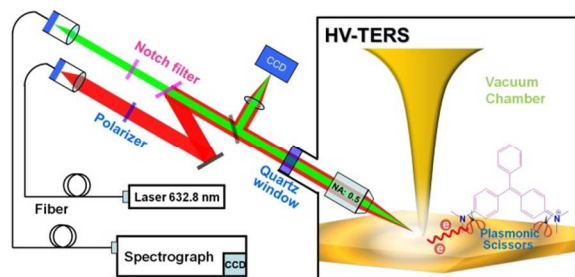
Fig. 1 Home-made setup of high-vacuum tip-enhanced Raman spectroscopy (HV-TERS) and mechanism of resonant dissociation by plasmonic scissors. Hot electrons are excited by laser light in the nanogap of a TERS setup tocut molecular bonds in the substrate-adsorbed Malachite Green molecules.

The method relies on the hot electrons and laser signal working in tandem. The laser assists to resonantly excite electronic transitions in molecular bonds in the MG. The hot electrons in turn provide the required energy to significantly overcome the reaction barrier and trigger the chemical reaction.[11, 16, 17, 20, 22, 23] Importantly, the lifetime of the hot electrons is on the order of femtoseconds, which is much shorter than the picosecond time scale of IVR. Furthermore, because the density of the hot electrons can be rationally controlled, via for example tuning of the laser signal, our methodology offers control of the rate and probability of the chemical reaction. Note that our resonant dissociative method relies on optical, rather than electrical means, as is the case in STM-related control of chemical reactions.[5, 6]

2 Experimental and theoretical methods

Vibrational spectra were measured with a home-built HV-TERS setup.[24-27] It consists of a homemade scanning tunneling microscope (STM) in a high vacuum chamber, a Raman spectrometer combined with a side illumination of 632.8 nm He-Ne laser light with an angle of 30° for Raman measurements, and three-dimensional piezo stages for the tip and sample manipulations. The objective is in the high vacuum chamber. The pressure in the chamber is about 10^{-7} Pa. A gold tip with the radius of about 50 nm was made by electrochemical etching of a 0.25 mm diameter gold wire.[28] The substrate was prepared by evaporating 100 nm silver film to a newly cleaned mica film under high vacuum. The film was immersed in a 1×10^{-5} M MG in ethanol solution for 24 hours, respectively, and then washed with ethanol for 10 minutes to guarantee that there was only one monolayer of molecules adsorbed on the silver film. Then the sample was immediately put into the high vacuum chamber. To get a good signal-to-noise ratio, the TERS signals were collected with an acquisition time of 20 seconds and accumulated 10 times for each spectrum on Ag film, and 40 seconds and accumulated 20 times for each spectrum on Au film. We also measured absorption spectrum of MG 10^{-2} M in water with absorption spectroscopy (HitachiU3010). SERS and SERRS spectra of MG were measured in Ag sol, using Leica microscopy equipment in a confocal Raman spectroscopic system (Renishaw, Invia), and the incident wavelengths are 785, 632.8 and 514.5 nm. The Ag sol for SERS measurement was synthesized, using Lee's method,[29] and the average diameter of nanoparticles is 80 nm.[10]

The theoretical simulations on Raman spectra were performed, using density functional theory,[30] B3LYP functional,[31, 32] 6-31G(d) basis for C, N, H atoms, and LANL2DZ basis[33] for Ag atom, which implemented in Gaussian 09.[34] These theoretical methods have been used to investigate Raman spectra in HT-TERS system, and which are rational theoretical methods. [35]

3 Results and discussion

The demonstration of the resonant dissociation of MG relies on several complementary experimental and theoretical investigations. Firstly, we measured optical absorption spectrum of MG (see Fig. 2(a)), which revealed that there is no any absorption peak at 785 nm, but there is a strong absorption peak around 632.8 nm, and a very weak absorption at 514.5 nm. Secondly, SERS spectra of MG in Ag sol were measured at these three frequencies (see Fig. 2(b)). It is normal Raman excited at 785 nm, and the Raman excited at 514 nm is similar with that excited at 785 nm; while it is resonance Raman excited at 632.8 nm, where Raman peaks A-D are selectively excited by resonance electronic transition at 632.8 nm, when the peak E is considered the normalized peak for comparison (the Figs of Raman without normalization can be seen from Fig. S1(a) in SI). Thirdly, our theoretical calculations identify that the peaks A-D related to vibrational modes in MG are associated with the –NC_2H_6 fragments (Fig. 2c). For MG, it is C_2 symmetry, and there are two kinds of vibrational modes a and b, and these five selectively enhanced vibrational modes were assigned as a_{39}, a_{45}, b_{49}, b_{61} and a_{58} from low to high frequencies. The simulated normal Raman spectrum of MG can be seen from Fig. S1(b), and the assignments of the normal Raman spectrum were listed in Table S1 in SI.

The peak E in Fig. 2(b) on the other hand is a vibrational mode associated with the C-C stretching mode of benzenyl. Consequently, our analysis shows that the energy of resonant excitation at 632.8 nm is concentrated on the modes A-D related to the –NC_2H_6 fragments. These modes can thus be selectively resonant excited. Note peaks B and C in Fig. 2(b) were superposed due to wide half high width, but they are well separated in HV-TERS in Fig. 3(a). By comparing TERRS excited at 632.8 nm and SERS excited at 785 nm, it is very clear that peaks A-D were selectively excited (see Fig.S1(c)).
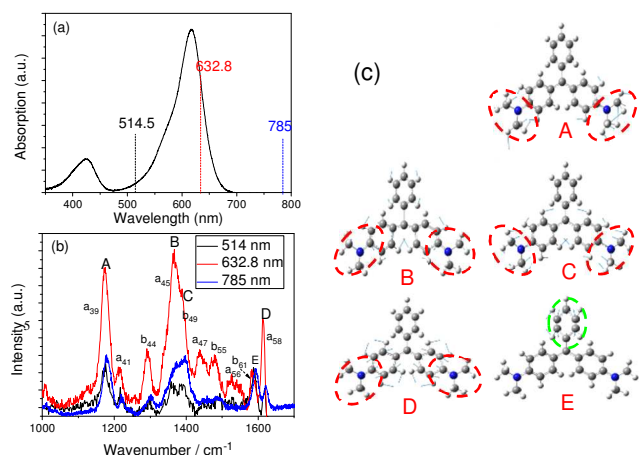
Fig. 2 Absorption and Raman spectra, and calculated normal modes of MG. (a) absorption spectrum of MG in water, (b) SERS and SERRS spectra of MG in Ag sol, (c) vibrational modes A-E of MG.

Now, we demonstrate the resonant dissociation process through time-dependent measurements using tip-enhanced resonance Raman spectroscopy (TERRS) in high vacuum at the incident light of 632.8 nm. Figs. 3(a)-(c) are time-sequential TERRS of MG adsorbed on Ag surface in high-vacuum in the presence of the incident light at 632.8 nm. At the initial stage, when the laser just radiates on the sample (t=0 minutes), the measured TERRS spectrum (Fig. 3a) shows that the Raman peaks A-D are strongly enhanced in TERRS by comparing with the off-resonance SERS spectrum excited at 785 nm (see Fig. S1(b) in SI), where the Raman peak E at 1592 cm^{-1} is used as the normalized peak in comparison. This means that the resonant excitation energies mainly selectively excite these four vibrational modes during the electronic transition. Our time-sequential TERRS measurements show evidence of a time-dependent molecular reaction dynamics process (Fig. 3a-c) that leads to a suppression of the peaks A-D and the emergence of new ones over time. Keeping the laser beam intensity constant over a period of time yields, at first, an increasingly complex, and unstable vibrational spectra (Fig. 3b) were obtained. After a period of *40 minutes* the spectrum stabilizes into the configuration shown in Fig. 2c. The strongly enhanced Raman peaks A-D that were initially present (Fig. 3a) are now not visible, whereas new peaks (denoted F-M in Fig. 3c) have emerged. The 2D plot of TER spectra (see Fig. 4) revealed that Fig. 3c is stabled final spectra in our experimental conditions. Fig. 3(d) and 3(e) are the simulated Raman spectra of dissociated fragments from MG, and the vibrational modes of them were also assignments, which can also be seen from Tables S2 and S3 in SI. The fragment of $HN(CH_3)$ is C_{2v} symmetry, there are four kinds of vibrational modes, a_1, a_2, b_1 and b_2. The large fragment in Fig. 3(d) is D_3 symmetry, while when it is attached to metal (see Fig. 3(f)), it is C_2 symmetry, and two kinds of vibrational modes *a* and b. The vibrational modes of them were also assigned in Fig. 3(d) and 3(e). The vibrational modes F-M in Fig. 3(c) can be seen from Fig. 3(f). The time-evolution of the TERRS spectra in Fig. 3 provides evidence for a dissociative chemical reaction taking place in MG. As the simulations of Raman spectra of the fragments of dissociation (Fig. 3d,e) clearly show, the final TERRS spectrum in Fig. 3c contains signatures from both dissociated fragments. It is important to estimate the ratio of chemical reaction in HV-TERS. There are about 157 molecules under the tip before reaction within effective 78 nm^2 (see discussion and Figure S2 in SI), where size of every molecule is about 0.5 nm^2. By comparing the intensity of peak C in Fig. 3(a) and Fig. 3(c), more than 60% of them have been dissociated by plasmon scissors. Also, by comparing the ratio of intensities of experimental and theoretical Raman peaks of G and I in Fig. 3(c), more than 40% molecules of $N(CH_3)_2$ are still present (another 20% molecules of $N(CH_3)_2$ were desorbed and pumped out of high vacuum chamber).
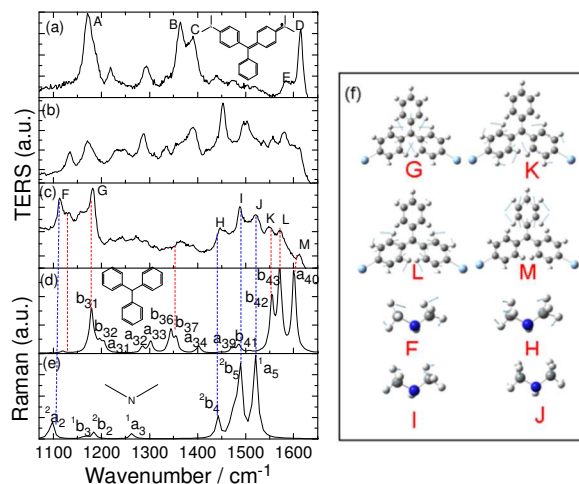
Fig. 3 Time sequential TERRS and the vibrational modes of MG. (a) The initial, (b) intermediate (20 minutes after continuous radiation by laser), and (c) the final spectra (40 minutes after continuous radiation by laser). The tunneling current and the bias voltage are 1 nA and 1V, respectively. (d, e) Simulated Raman spectra of fragments (see the insets). (f) The vibrational modes of dissociated fragments of MG (corresponding to the experimental peaks in Fig. 3(d)-(e) as calculated by density functional theory).
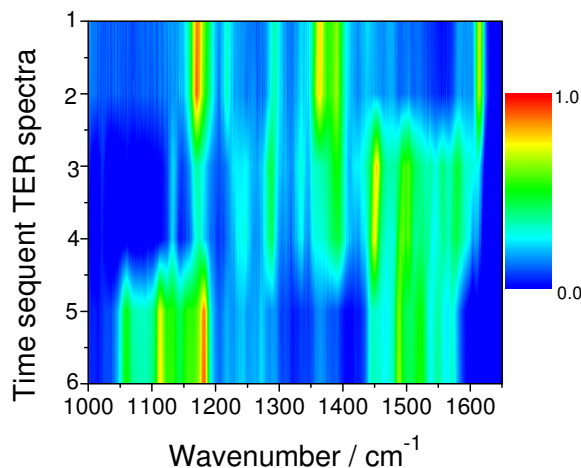
Fig. 4 Time sequent TER spectra, and the color bar is shown in the right of figure. The time interval is 20 minutes for each TER spectrum.

We also made similar observations also for MG adsorbed on Au film (see Fig. 5). Note that Fig. S2 in SI, which is also measured after 40 minutes, similar to the results in Fig.3b, displays evidence for a partial reaction since peaks A-C are not completed vanished yet compared to Fig. 3c, even though the new peaks F-M have appeared. We therefore conclude that the chemical reaction on Au substrate is slower than that on Ag film.
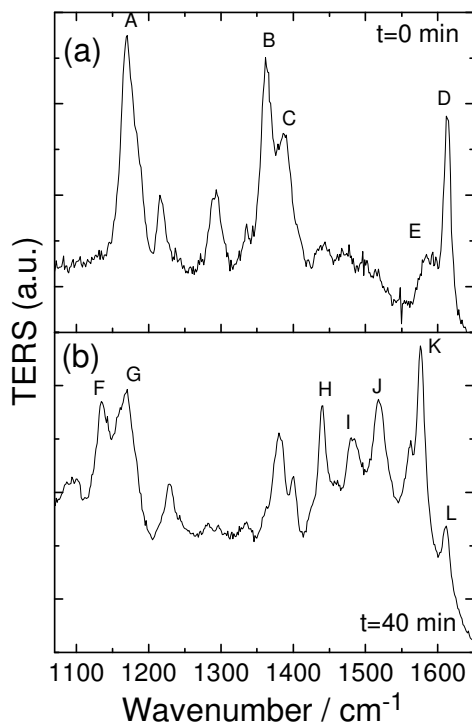
Fig. 5 Time sequential TERRS and the vibrational modes of MG adsorbed on Au film. (a) The initial, and (b) the spectra at 40 minutes after continuous radiation by laser). The tunneling current and the bias voltage are 1 nA and 1V, respectively.

Note that we believe the process of electrons transfer should be in the time scale of femtoseconds, if hot electrons have successfully attached to molecules. While, there is a probability that how may hot electrons can successfully attached to molecules, which strongly dependent on the density of electrons. Plasmon intensity along substrate is highly asymmetric, when away from the center, the plasmon intensity is weaker. So, the reaction time of all molecules within effective 78 nm^2 (see SI) in the effect region is not simultaneously. So far from the center, the plasmon intensity is weak, and then the density of hot electrons is weaker. So, the probability of electrons successfully attached to molecules is also smaller, compared with the reaction at the center of gap, and therefore, the chemical reactions are slower than those at the center of nanogap.

The rate and probability of chemical reaction can be controlled by varying the tunneling current, bias voltage and laser intensity in HV-TERS. In our method, the most natural way of controlling rate and probability of dissociation is by changing the plasmon intensity via tuning of the laser intensity.[16] As demonstrated in

Fig. 6(a)-(b), a decrease of the laser power by 10% of the total laser power yields a much slower dissociation rate – after 40 minutes, the spectra in Fig. 6d is far from the stable configuration in Fig. 3c. The strongly enhanced Raman peaks A-C that were still visible, though new peaks have emerged (see Fig. 6b).
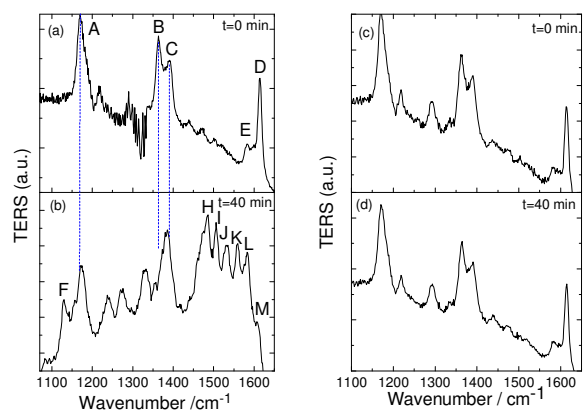
Fig. 6 TERRS of MG adsorbed on Ag film at t=0 and t=40 minutes. (a)-(b) sample irradiated with 10% lower laser power compared to the sample analyzed in Fig. 2a and 2c shows a evidence for a slower dissociation rate, and, (c)-(d) without continuous laser-irradiation of the sample shows that the tunneling current alone is not sufficient to induce dissociation.

To elucidate the origin of the observed dissociation, we have performed additional measurements to evaluate the contribution of the tunneling current to the resonant dissociation process. Previous reports have shown that chemical bonds can be broken or formed by tunneling electron currents or bias voltages alone.[5, 6, 29, 30] Our measurements and analysis show that this is not the case in our study Measurements of TERRS spectra at t=0 and t=40 minutes, without the irradiation of the sample by laser light there between, and at a constant tunneling current, show that the profiles of the two TERRS spectra are identical (see Fig. 6 (c)-(d)). Consequently, the energy provided by the laser and the tunneling current is not large enough to dissociate the molecules, unless the laser continuously irradiates the sample to provide a continuous supply of a large density of hot electrons.

The physical origins for the resonant dissociation rely on the generation of hot electrons. Large densities of plasmons are first produced by the laser irradiation of the nanogap between the tip and substrate in the HV-TERS. Hot electrons with high kinetic energy are then generated from the plasmon decay, and work in tandem with the laser beam to induce the dissociation process (see Fig. 7). The resonant electronic transition increases the lifetime of the Raman scattering (compared to the normal Raman scattering), and the resonant excitation by the laser results in the excitation energy concentrating on the vibrational modes associated with the $-NC_2H_6$ fragments of MG, thereby selectively weaken these bonds (process A in Fig. 7). The hot electrons generated from the plasmon decay in turn serve two purposes: First, because of their high kinetic energy, when the hot electrons impinge on the metal-adsorbed molecules, they induce a change of the molecules' excited-state potential energy surface (ESPES) from a neutral to a temporarily negative ion excited state (ESPES$^-$) (process B in Fig. 7). The redox state due to the hot electron is a

transient negative state.[31]

Second, the kinetic energy is transferred from the hot electrons to the intra-molecular vibrational dissociation energy during their interactions (process C in Fig. 7). Both of these processes lead to an effective overcoming of the energy barrier (Fig. 7) for the chemical reaction to take place - either by overcoming or tunneling through the barrier such that the reaction leading to dissociation can occur. Note that in our experiment, to keep stable the B and C components of the total energy required by the chemical reaction, we have to irradiate the sample continuously by the laser to sustain a large density of hot electrons. It is a process of multi-electron driven. Note that hot electrons donating their energy to the molecule is not necessarily bond-selective. In short, this process in Fig. 7 is resonant Raman to selectively weaken the bond, followed by dumping in lots of indiscriminant energy and breaking these active weakest bonds. So, the bond broken is not simply the lowest energy one available, but actually was induced selectively.

Furthermore, the laser intensity, tunneling current or bias voltage in the HV-TERS may also provide further energy for the dissociation. This allows for control of the rate and probability of dissociation. As shown in Fig. 6, decreasing the laser intensity leads to a slower dissociation rate and probability. This is because the decrease in the laser intensity leads to a decrease in the plasmon intensity, which in turn determines the density of hot electrons. It should be noted that the diagram in Fig. 7 is qualitative. The energy of hot electrons generated from plasmon decay may be less than that of photon, if these hot electrons relaxed before reacting; otherwise, it is just as large as the photon as well.
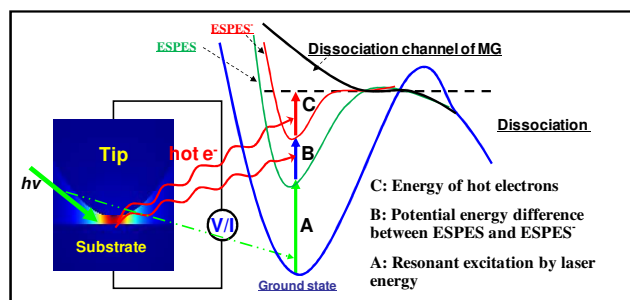
Fig. 7 The mechanism of resonant dissociation by plasmon scissors. Three main energetic components drive the chemical reaction: A: resonant absorption of the laser light enhances the vibrational modes associated with $-NC_2H_6$ and excites the MG molecules to an excited-state potential energy surface (ESPES); B: hot electrons temporarily change the molecules' ESPES from a neutral to a negative ion excited state (ESPES$^-$); C: the kinetic energy of the hot electrons is converted to intramolecular vibrational thermal energy.

4 Conclusion

In conclusion, our study not only demonstrates the plasmonic scissor concept as an efficient tool for resonant control of dissociation of surface-adsorbed molecules, but establishes the concept of plasmonic hot-electron mediated chemistry as an important new field extending the reach of photochemistry to chemical reactions where simple photon absorption does not suffice, but where the additional energy supplied by hot electrons generated by SPs yields the necessary means of control. It also demonstrates that HV-TERS is a promising technique for in situ surface chemical analysis and manipulation on the nanoscale.

Notes

[a] Beijing National Laboratory for Condensed Matter Physics, Institute of Physics, Chinese Academy of Sciences, P. O. Box 603-146, Beijing, 100190, People's Republic of China. E-mail: mtsun@iphy.ac.cn.
[b] School of Physics and Information Technology, Shaanxi Normal University, Xi'an, 710062, People's Republic of China.
[c] Leibniz Institute of Photonic Technology, Albert-Einstein-Str. 9, 07745, Jena, Germany.

† Electronic Supplementary Information (ESI) available: [Further experimental spectra and theoretical calculations.]. See DOI: 10.1039/b000000x/

References

1 F. F. Crim, Proc. Natl. Acad. Sci. USA 2008, 105, 12654-12661.
2 A. Assion, T. Baumert, M. Bergt, T. Brixner, B. Kiefer, V. Seyfried, M. Strehle, G. Gerber, Science 1998, 282, 919-922.
3 T. Uzer, W. H. Miller, Phys. Rep. 1991, 199, 73-146.
4 D. R. Killelea, V. L. Campbell, N. S. Shuman, A. L. Utz, Science 2008, 319, 790-793.
5 J. R. Hahn, W. Ho, J. Chem. Phys. 2009, 131, 044706 (1-4).
6 Y. Jiang, Q. Huan, L. Fabris, G. C. Bazan, W. Ho, Nature Chem. 2013, 5, 36-41.
7 M. W. Knight, H. Sobhani, P. Nordlander, N. J. Halas, Science 2011, 332, 702-704.
8 (a) Z. L. Zhang, L. Chen, M. T. Sun, P. P. Ruan, H. R. Zheng, H. X. Xu, Nanoscale 2013, 5, 3249-3249; (b) Z. L. Zhang, M. T. Sun, P. P. Ruan, H. R. Zheng, H. X. Xu, Nanoscale 2013, 5, 4151.
9 K. Watanabe, D. Menzel, N. Nilius, H. J. Freund, Chem. Rev. 2006, 106, 4301-4320.
10 Y. R. Fang, Y. Z. Li, H. X. Xu, M. T. Sun, Langmuir 2010, 26, 7737-7746.
11 P. Christopher, H. L. Xin, S. Linic, Nat. Chem. 2011, 3, 467-472.
12 S. Linic, P. Christopher, D. B. Ingram, Nat. Mater. 2011, 10, 911-921.
13 H. P. Zhu, G. K. Liu, D. Y. Wu, B. Ren, Z. Q. Tian, J. Am. Chem. Soc. 2010, 132, 9244-9246.
14 (a) M. T. Sun, H. X. Xu, Small 2012, 8, 2777-2786. (b) M. T. Sun, Z. L. Zhang, P. J. Wang, Q. Li, F. C. Ma, H. X. Xu, Light: Science & Applications, 2013, 2, e112.
15 L. Brus, Acc. Chem. Res. 2008, 41, 1742-1749.
16 (a) M. T. Sun, Z. L. Zhang, H. R. Zheng, H. X. Xu, Sci. Rep. 2012, 2, 647 (1-4); (b) M. T. Sun, Y. R. Fang, Z. Y. Zhang, H. X. Xu, Phys. Rev. E 2013, 87, 020401.
17 S. Mukherjee, F. Libisch, N. Large, O. Neumann, L. V. Brown, J. Cheng, J. B. Lassiter, E. A. Carter, P. Nordlander, N. J. Halas, Nano Lett 2013, 13, 240-247.
18 H. Kim, K. M. Kosuda, R. P. Van Duyne, P. C. Stair, Chem. Soc. Rev. 2010, 39, 4820-4844.
19 E. M. V. Lantman, T. Deckert-Gaudig, A. J. G. Mank, V. Deckert, B. M. Weckhuysen, Nat. Nanotechnol. 2012, 7, 583-586.

20 M. T. Sun, Z. L. Zhang, Z. H. Kim, H. R. Zheng, H. X. Xu, Chem. Eur. J. 2013, 19, 14958.
21 K. Kim, K. L. Kim, K. S. Shin, Langmuir 2013, 29, 183-190.
22 S. Linic, P. Christopher, H. Xin, Acc. Chem. Res. 2013, 46, 1890-1899.
23 P. Christopher, H. Xin, A. Marimuthu, S. Linic, Nat. Mater. 2012, 11, 1044–1050.
24 M. J. Frisch, et. al, Gaussian 09 revision A. 02. Wallingford CT: Gaussian Inc., 2009.
25 M. T. Sun, Z. L. Zhang, L. Chen, H. X. Xu, Adv. Optical Mater. 2013, 1, 449–455.
26 M. T. Sun, Z. L. Zhang, L. Chen, S. X. Sheng, H. X. Xu, Adv. Optical Mater. 2014, 2, 74-80.
27 Z. L. Zhang, X. R. Tian, H. R. Zheng, H. X. Xu, M. T. Sun, Plasmonics, 2013, 8(2):523-527
28 B. Ren, G. Picardi, B. Pettinger, Rev. Sci. Instrum. 2004, 75, 837-841.
29 H. J. Lee, W. Ho, Science 1999, 286, 1719-1722.
30 S. W. Hla, K. H. Rieder, Annu. Rev. Phys. Chem. 2003, 54, 307-330.
31 K. H. Kim, K. Watanabe, D. Mulugeta, H.-J. Freund, D. Menzel, Phys. Rev. Lett. 2011, 107, 047401(1-4).
32 P. C. Lee, D. Meisel, J. Phys. Chem. 1982, 86, 3391-3395.
33 P. Hohenberg, W. Kohn, Phys. Rev. B 1964, 136, B864-B671.
34 C. T. Lee, W. T. Yang, R. G. Parr, Phys. Rev. B 1988, 37, 785-789.
35 A.D. Becke, J. Chem. Phys. 1993, 98, 5648-5652.
36 P. J. Hay, W. R. Wadt, J. Chem. Phys. 1985, 82, (1), 270-283.

Nanoscale Accepted Manuscript